MATERIALS CHEMISTRY FRONTIERS

Triphenylamine based Donor – π – Acceptor Organic Phosphors: Synthesis, Characterization and Theoretical study

Journal:	*Materials Chemistry Frontiers*
Manuscript ID	QM-RES-04-2016-000031.R2
Article Type:	Research Article
Date Submitted by the Author:	21-Jul-2016
Complete List of Authors:	Kajjam, Aravind; NIT, Chemistry Giri, Santanab; NIT, Chemistry Vaidyanathan, Sivakumar; National Institute of Technology, Chemistry

Journal Name

ARTICLE

Triphenylamine based Donor – π – Acceptor Organic Phosphors: Synthesis, Characterization and Theoretical study

Received 00th January 20xx,
Accepted 00th January 20xx

DOI: 10.1039/x0xx00000x

www.rsc.org/

Aravind Babu Kajjam, Santanb Giri and Sivakumar V.*

Abstract: We have designed and synthesized donor (D) and acceptor (A) phosphors [D and A refer to the electron-donating and electron-withdrawing moieties, respectively] as yellow-emitting organic phosphors. The photophysical and electrochemical properties of the phosphors have been studied in details. The UV-Vis spectra of the organic phosphors show multiple absorption bands (UV to near UV region, due to π - π* transitions of conjugated chain) and all the phosphors are showing yellowish-green/yellow (556, 576, 594 nm) emission with appropriate Commission Internationale de l'Eclairage (CIE) color coordinates values. In contrast, bathochromic shift were observed in the solid-state emission spectra for the one donor two acceptors and one donor three acceptors due to the π – π interaction and aggregation induced emission. The electrochemical studies were carried out to find the HOMO, LUMO and band gap of the phosphors and verified the same by density functional theory (DFT) calculations. By using time dependent - DFT (TD - DFT) calculations singlet and triplet energy levels also calculated. In addition, solvatochromism studies also been carried out and the results are interpreted by using Lippert–Mataga equation. White light can be realized from the currently synthesized organic yellow phosphors integrated with blue LEDs or blue fluorophores.

Introduction

Phosphors are active components in light-emitting diodes (LEDs) have attracted widespread interest in over the decades. White LEDs & OLEDs (WLEDS, solid state lighting) technology advance towards trading of existing less efficient and environmentally begin technologies such as incandescent and fluorescent lamps [1]. In comparison with traditional lightings, the InGaN-based WLEDs have many advantages in energy efficiency, long lifetime, compactness, environment friendliness and designable features [2]. The wavelength converting phosphor materials play a vital role for the creation of white light from LEDs (solid-state lighting). Several approaches are available to mimic white light from LEDs: first, a combination of an InGaN-based blue LED chip with a yellow phosphor (e.g., YAG:Ce^{3+} based materials); second, a blue LED chip combined with a green and a red emitting phosphor instead of single yellow emitting phosphor [3,4] These two phosphors absorb partial blue light from InGaN chip and convert into green and red photons and produce white light by complementary color mixing. Research efforts have been directed over a decade for the improvement or find new wavelength convertors for potential applications in WLEDs. The concept of using the remote phosphors are exciting (i.e) the combination of the near UV or blue LED chip and RBG or yellow phosphor in an appropriate distance [5]. This technology (remote-type phosphor-LEDs) will help to overcome some high-tech limitations that includes thermal quenching of organic phosphors, light extraction efficiency and light distribution within remote-type designed packaging. However, most of the efforts have been faithful to inorganic phosphors such as YAG:Ce^{3+}, M_2Si_5N8 (M = Ca, Sr, Ba), $Sr[LiAl_3N_4]:Eu^{2+}$, $BaLa_2Si_2S_8:Eu^{2+}$, $K_2TiF_6:Mn^{4+}$ and $Ca_5(SiO_4)_2F_2:Eu^{2+}$ [6,7] in which the key concerts are yet to be improved for practical applications, i.e. high cost, difficulties in color tuning and un-uniform dispersion [8] Whereas, organic color conversion phosphor material offer significant advantages, such as low manufacturing cost and structural flexibility, their use as white light sources is limited by their generally lower efficiency when compared with their inorganic LED counterparts. One of the interesting paths to develop WLED is through a hybrid inorganic/organic LED architecture, where a blue emissive inorganic LED is coated with an organic material that has an absorbance band aligned with the emission wavelength of the inorganic LED structure [9-11]. The organic phosphor material acts as an energy down-converter for the inorganic LEDs, converting some of the emitted high energy blue photons to lower energy yellowish red light. The mixing of both blue and yellowish red delivers a high quality white output (warm white light). The material system of choice for the inorganic LED is the III-nitride alloy system, which can emit light from the ultraviolet (UV), through the visible to infrared spectrum [12]. Such hybrid inorganic/organic LED architectures offer the potential to combine the advantages of both technologies, for example, the excellent electronic properties of inorganic substrates and the broad, tunable emission of organic phosphors [13-16]. Additionally, employing an organic phosphor material in place of traditional phosphors in hybrid LEDs would avoid an industry dependency on costly rare-earth containing materials as demand for development of solid-state lighting [17]. The higher speed of response of the organic materials compared to the existing phosphors offer additional advantages which are used in visible light communications [18, 19]. Design and synthesis of highly efficient organic phosphors are key determinants in the performance of the hybrid white LEDs. Organic phosphors typically possess strong absorptions in near UV to blue region (where the LED emission occurs), which are caused by π-π* transitions. It is possible to tune the emission color gamut by changing the molecular design and structural modifications of the organic phosphors [20].

In general, white emission in OLEDs is typically generated from multiple emitters to cover a wide range of spectral window, e.g. the whole visible region from 380 to 680 nm. Recent prototypes of WOLEDs have even been benefiting from favorable features, such as homogenous large-area emission, and being lightweight and ultra-thin. In the case of lighting applications, WOLEDs are expected to achieve low energy consumption, long lifetime and low cost to compete with other light sources such as

*Department of Chemistry, National Institute of Technology, Rourkela, 769008, India. *corresponding author: E-mail: vsiva@nitrkl.ac.in*
†Electronic Supplementary Information (ESI) available: See DOI: 10.1039/x0xx00000x

fluorescent tubes and inorganic LEDs. In order to improve the efficiency as well as color purity of the WOLEDs to consider for commercial application, lot of efforts have been made, which includes more emphasis on developing efficient and stable materials. Till date, three primary color strategies (mixing of RGB) is superior because it is easier to reach white light with Commission Internationale de l'Eclairage (CIE) coordinates, due to simultaneous presence of the three primary colors. However, the efficiency of the device with primary colors is low due to high operational voltages and unexpected spectral variations due to recombination zone shift [21]. In general, aggregation induced emission (AIE) is another process which is associated with chromophore aggregation [22]. In this process weekly luminescent chromophores are induced to emit efficiently in aggregate state [23]. This phenomenon is useful towards efficient solid-state light emitters, bioprobes, chemosensors, and smart materials [22]. To further improve the efficiencies of device as well as the color purity, it is necessary to develop novel blue and yellowish-orange emitters with high luminescent efficiency. In order to accomplish the above stated advantages, we have designed and synthesized a group of 1-phenylethanone decorated triphenylamine conjugated organic phosphors for White OLEDs. In general, most of the sensitizers that have been designed and developed with a D–π-bridge–A dyad structure [24]. Triphenylamine, coumarin, and indoline [25] are examples of electron donating building blocks that provides high stability and suitable for device fabrication. In that, Triphenylamine as the molecule core to construct branched molecules due to its excellent electron donating ability (D) and variable star-shaped structure.[26] In spite of the large availability of donating groups, the selection of acceptors remains fairly short. During our search for acceptor structures, we came across a previous report on dibenz[a,c]phenazine (DBP) derivatives [27], which demonstrated their high light absorptivity and their suitable frontier orbital energies levels for application in dye sensitized solar cells (DSSCs). The systems with extended π-electrons and small reorganization energy provides a good route to enhance charge separation lifetimes, DBP is an interesting choice as a fused D–A core for organic phosphors. Keeping this in mind we have designed and synthesized one donor - one acceptor (D – π-bridge – A), one donor - two acceptors (A– π-bridge – D– π-bridge – A) and one donor – three acceptors (D– π-bridge – A(– π-bridge – D) – π-bridge – D) groups, where D and A refer to the electron-donating and electron-withdrawing moieties, respectively. Therefore, the target molecule with high intense light emission under near UV excitation is expected.

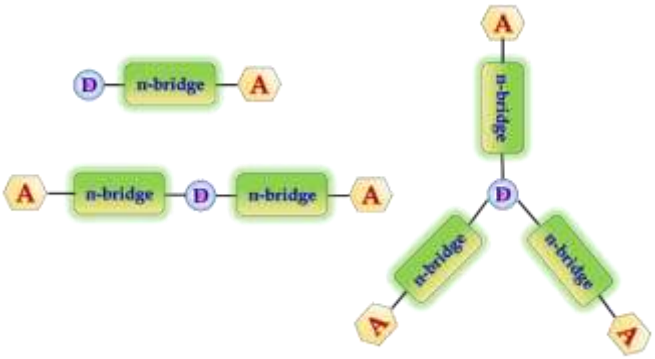

Fig.1. Designed donor - (π-bridge) – acceptor molecules.

In this study, we report on the synthesis and characterization of triphenylamine-based phosphors with multiple electron acceptors of 1-phenylethanone. In the molecular design, (E)-3-(4-(diphenylamino)phenyl)-1-phenylprop-2-en-1-one (FTPA-Acetophenone = formyl triphenylamine-acetophenone) is the basic model [32], in which the TPA unit was connected to one molecule of 1-phenylethanone. In the second case, 1-phenylethanone was introduced to the adjacent phenyl ring of FTPA, to obtain DFTPA-Acetophenone (diformyl triphenylamine-Acetophenone) that has two electron acceptors. Similarly, in the third case 1-phenylethanone was attached to the third phenyl ring of FTPA, yielding the structure of TFTPA-Acetophenone (triformyltriphenylamine-acetophenone). The introduction of multiple electron acceptors to the adjacent phenyl ring of TPA-based phosphors would have a significant influence on the efficiency and brightness of the LEDs. The phosphors were characterized by proton and carbon NMR, DTA-TGA analysis and powder X-ray diffraction. The photophysical studies were also carried out by using UV-visible, photoluminescence spectroscopy (including solvatochromism) and verified the spectral data's theoretically (DFT and TD-DFT). The electrochemical studies were carried out to find the energy gap (HOMO – LUMO gap) and the same is verified by density functional theory calculation. From the emission spectral values the Commission International del'Eclairage (CIE) has also been calculated by using MATLAB software.

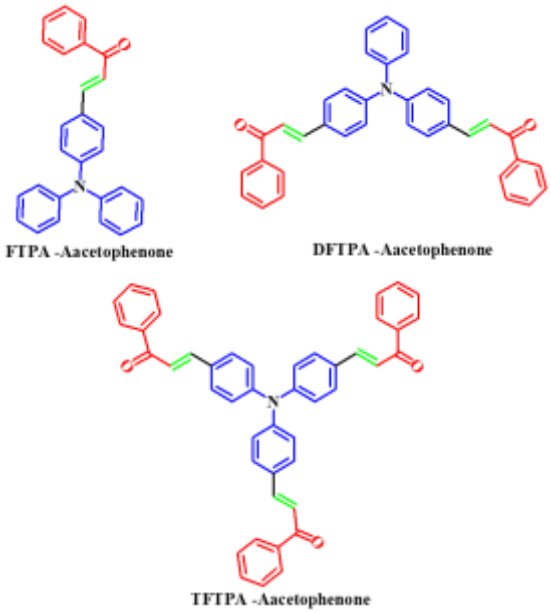

Fig.2. Chemical structure of TPA substituted Acetophenones.

Experimental session

General information:

^{1}H-NMR spectra were measured on a BRUKER AV 400 Avance-III (400MHz) instrument with tetramethylsilane as the internal standard. Absorption and photoluminescence excitation and emission spectra of the target compound were measured using SHIMADZU UV-2450 spectrophotometer and HORIBA FLUOROMAX - 4P spectrophotometer, respectively. Absolute quantum yield of the synthesized phosphors determined by using quinine sulfate in 1M H_2SO_4 (Φ = 0.546). Thermogravimetric analysis (TGA) was performed on a NETZSCH - Germany thermal analyzer under nitrogen atmosphere at a heating rate of 10°C min^{-1}. Cyclic voltammetry experiment was performed in dimethylformamide solution containing 0.1 M tert-butylammonium perchlorate using Ag/AgCl as the reference electrode at a scan rate of 100 mV s^{-1} using AUTOLAB 302N Modular potentiostat. Elemental analysis of synthesized phosphors has been measured by using Elementar Analysen Systeme, Germany/Vario EL. The CIE color chromaticity coordinates of the phosphor has been calculated from the emission spectral values by using MATLAB software. Powder X-ray diffraction of phosphors were measured by X-ray powder diffraction (XRD) using Cu-Kα1 radiation (Rigaku, ULTIMA IV) in the 2θ range from 5 to 60°. All the measurements were carried out at room temperature (RT).

Computational details:

The molecules under study were first optimized in the gas phase using density functional theory and Becke three parameter Lee-Yang-Parr (B3LYP) [28] form for exchange-correlation potential and 6-31G (d, p) basis set. All the structures were found to be in the minima of the potential energy surface as the normal mode of frequencies are all positive. After that we performed the UV−Vis spectra calculation using time dependent density functional theory (TD-DFT) [29] with gas phase optimized geometries. It is expected that the geometry of the molecule will change in solvent phase in comparison to that of the gas phase and hence the optimization of the geometries under solvent phase has also been carried out. We have found that there is no

such prominent change in the geometries of the molecule. As the UV-Vis experiment was done in solution phase, we also calculated the UV–Vis spectra in solvent by using the polarizable continuum model (PCM)[30] approach within the TD-DFT methodology. Singlet and triplet energy calculations are done by using TD-SCF and B3LYP/6-31G(P)approach. All calculations were carried out using Gaussian09 W [31] and GaussianView suite of programs.

Materials:

All reagents were used as purchased without any further purification. All operations involving air-sensitive reagents were performed under a dry nitrogen atmosphere. 4-formaltriphenylamine (FTPA), 4, 4′-diformaltriphenylamine (DFTPA), 4, 4′, 4′′-triformaltriphenylamine (TFTPA), were prepared according to literature procedures [27] and the target organic phosphors synthesized by using aldol condensation procedure [32]. All the phosphor materials are soluble in common organic solvents, such as toluene, tetrahydrofuran (THF), dichloromethane (DCM), Chloroform, acetonitrile, acetone and N,N-dimethylformamide (DMF), Methanol (MeOH) but are insoluble in water.

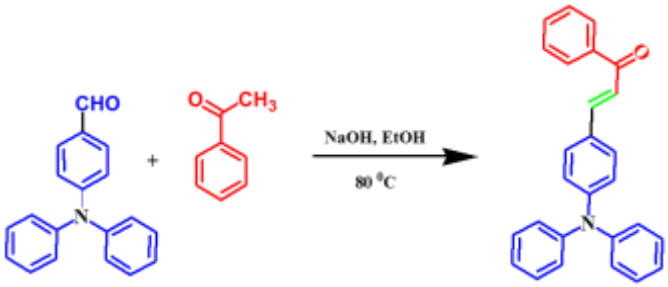

Scheme 1. Synthesis of TPA substituted yellow phosphors.

Synthesis of FTPA: Dimethylformamide (DMF) (1.71 mL, 22.04 mmol) was taken in a clean-dried two neck round bottom flask and added drop wise phosphorous oxy chloride (2.05 ml, 22.04 mmol) at 5°C. After 30 min, triphenylamine (TPA) (2 g, 8.163 mmol) in DMF 22 (15 mL) was added drop wise to reaction mixture at same temperature. The resulting mixture was stirred for overnight at RT, then poured into water and neutralized with diluted sodium hydroxide solution (up to pH 6). Then extracted with chloroform and washed with brine solution followed by dried with sodium sulphate. The crude product was washed with diethyl ether : hexane (3:7) mixture solvent and recrystallized in ethanol to get pure (90%) pale yellow colored fine solid. ^{1}H-NMR Data ($CdCl_3$, 400MHz): δ = 9.82 (s, 1H), 7.70 (d, 2H), 7.38-7.34 (m, 2H), 7.25-7.24 (m, 2H), 7.20-7.15 (m, 6H), 7.03 (d, 2H). ^{13}C-NMR Data (CDCl3, 100MHz): δ = 153.3, 146.1, 131.3, 129.7, 129.0, 126.3, 125.1, 119.3.

Synthesis of DFTPA: Phosphorus oxychloride (3.74 mL 39.98 mmol) was added dropwise at 0°C under N_2 to DMF (4.08 mL, 27.95 mmol) and the reaction mixture was stirred for 1 h. Triphenylamine (1 g, 4.0816 mmol) was added, and the resulting mixture was stirred at 105°C for 4 h. After cooling to RT, the mixture was poured into ice water slowly, whereby a brown solid precipitated out. The solid was filtered, washed with water. The crude product was purified by column chromatography (CH_2Cl_2/Hex =1: 3) to yield (81%) as a yellow solid. ^{1}H NMR data ($CdCl_3$, 400MHz): δ = 9.90 (s, 2H), 7.77 – 7.80 (d, 4H), 7.39 – 7.43 (t, 2H), 7.25 – 7.29 (t, 1H), 7.20 – 7.21 (d, 6H). ^{13}C NMR data ($CDCl_3$, 100MHz): δ = 190.56, 151.20, 132.56, 131.53, 131.34, 128.80, 127.09, 124.54, 122.77.

Synthesis of TFTPA: Phosphorus oxychloride (8.01 mL 85.71 mmol) was added dropwise at 0°C under N_2 to DMF (4.69 mL, 60.44 mmol) and the reaction mixture was stirred for 1 h. Triphenylamine (1 g, 4.0816 mmol) was added, and the resulting mixture was stirred at 105°C for 4 hrs. After cooling to RT, the mixture was poured into ice water slowly, whereby a brown solid precipitated out. The solid was filtered, washed with water. The crude product was purified by column chromatography (CH_2Cl_2/Hex =1: 3) to yield (38%) as a bright yellow solid. ^{1}H NMR data: δ = 9.96 (s, 3H), 7.77 – 7.87 (d, 6H), 7.14 – 7.277 (d, 6H). ^{13}C NMR data ($CDCl_3$, 100MHz): δ = 191.31, 152.14, 133.73, 132.04, 125.48.

Synthesis of phosphor material: Aldehyde (1.831 mmol, 1eq) and NaOH (1.831 mmol, 1 eq) were added into the mixture of 30 mL of water and 25 mL of ethanol, then 1-phenylethanone (3.663 mmol, 2eq) was added. The mixture was heated and stirred at 90°C for 4 hrs. After cooling, the mixture was filtered and washed with plenty of water and then dried up at RT to produce yellow powder with yield of 80%.

FTPA-Acetophenone: ^{1}H NMR data: δ = 8.01 (d, 2H), 7.77 (d, 1H), 7.58–7.54 (t, 1H), 7.51–7.48 (m, 4H), 7.39 (d, 1H), 7.33–7.30 (t, 4H), 7.18–7.09 (m, 6H), 7.04 (d, 2H). ^{13}C NMR data ($CDCl_3$, 100MHz): δ = 195.26, 143.29, 137.13, 134.39, 134.16, 133.20, 133.05, 132.46, 130.14, 128.78, 126.20, 124.06. Anal. calcd for $C_{27}H_{21}NO$: C, 86.37; H, 5.64; N, 3.73; O, 4.26 Found: C, 86.27; H, 5.59; N, 3.71; O, 4.23.

DFTPA-Acetophenone: ^{1}H NMR data: δ = 8.02 – 8.04 (d, 2H), 7.74 – 7.84 (m, 4H), 7.58 – 7.61 (m, 2H), 7.54 – 7.56 (m, 3H), 7.47 – 7.48 (d, 1H), 7.37 – 7.44 (m, 3H), 7.18 – 7.21 (m, 9H), 7.13 – 7.16 (m, 2H). ^{13}C NMR data (CDCl3, 100MHz): δ = 195.29, 148.67, 137.43, 137.33, 136.00, 135.87, 134.82, 134.48, 133.30, 133.10, 131.73, 130.94, 129.32, 128.02, 127.41, 125.88. Anal. calcd for $C_{36}H_{27}NO_2$: C, 85.52; H, 5.38; N, 2.77; O, 6.33 Found: C, 85.49; H, 5.32; N, 2.71; O, 6.30.

TFTPA-Acetophenone: ^{1}H NMR data: δ = 8.031 -8.049 (d, 6H), 7.77 – 7.87 (m, 4H), 7.59 – 7.69 (m, 6H), 7.48 – 7.64 (m, 8H), 7.27 (d, 2H), 7.19 – 7.21 (t, 3H), 7.11 (d, 2H). ^{13}C NMR data ($CDCl_3$, 100MHz): δ = 194.92, 142.98, 137.35, 136.06, 134.58, 134.51, 132.75, 129.13, 128.06, 127.21, 126.30. Anal. calcd for $C_{45}H_{33}NO_3$: C, 85.01; H, 5.23; N, 2.20; O, 7.55 Found: C, 85.10; H, 5.16; N, 2.15; O, 7.51.

Results and Discussion

Thermal properties:

Differential thermal analysis (DTA) and thermogravimetric analysis (TGA) of the phosphors were carried out simultaneously by employing NETZSCH thermal analyzer. The sample was heated at a rate of 10°C/min in nitrogen atmosphere. TG-DTA curves of synthesized phosphors are depicted in Fig. 3. In the DTA curve of FTPA-Acetophenone, the first endothermic peak observed at 274°C and it is attributed to the meting point of the sample. Another important observation is that, there is no phase transition till the material melts and this enhances the temperature range for the utility of the LED applications. Presence of water of crystallization in the molecular structure was indicated by the presence of the weight loss near 125°C. Further there was no decomposition near the melting point. This ensures the suitability of the material for possible application in LEDs, where the phosphor materials are required to withstand high temperatures (~125°C). The weight loss starts around 138°C and the weight loss corresponding to decomposition of phosphor was observed at 350°C, which takes place over large temperature range (138–350°C) where almost all the gaseous fragments like carbon dioxide and ammonia might be liberated. The TGA reveals exactly the same changes shown by DTA.

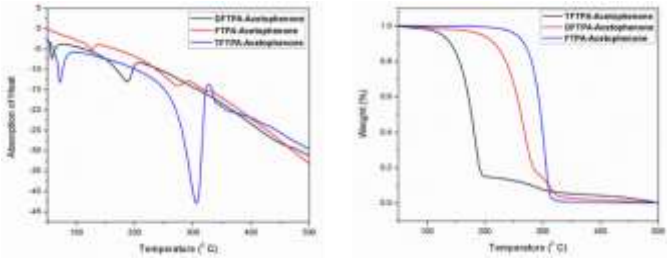

Fig.3. a) DTA curves of yellow phosphors. b) TGA curves of yellow phosphors.

The second endothermic peak in the DTA curve shows that the phosphor material is fully decomposed at 318°C. The sharpness of the endothermic peak shows good degree of crystallinity of the grown sample. The weight loss temperatures of the DFTPA-Acetophenone and TFTPA-Acetophenone phosphors were 57, 375°C and 70, 450°C, respectively. The temperatures of

decomposition (Td: corresponding to 5% weight loss) of DFTPA-Acetophenone and TFTPA-Acetophenone are 187°C and 306°C, respectively. However, the corresponding temperature ranges of DFTPA-Acetophenone and DFTPA-Acetophenone phosphors with the same weight loss are 57 – 375°C and 70 – 450°C, respectively. The thermal properties of the currently synthesized yellow phosphors are virtuous for the normal operating conditions of remote-type phosphor (40 – 90°C) based LEDs [33].

Powder XRD studies:

XRD patterns of the synthesized yellow phosphors are shown in Fig 4. The FTPA-Acetophenone shows in crystalline nature, whereas the diffraction peaks of DFTPA and TFTPA-Acetophenone shows amorphous phase. It clearly indicates that successive addition of acceptor groups in the TPA moiety, the crystalline nature of the FTPA-Acetophenone changes to amorphous nature. In general, amorphous luminophores are highly required to fabricate the solution processable OLEDs, wherein the luminophore should not crystalline in the device operating conditions. In general, amorphous behavior is achieved by introduction of bulky substituents which hinder the packing of the molecules. The currently synthesized phosphor materials are shown potent to be used as a phosphor for solution processable white organic light emitting diodes.

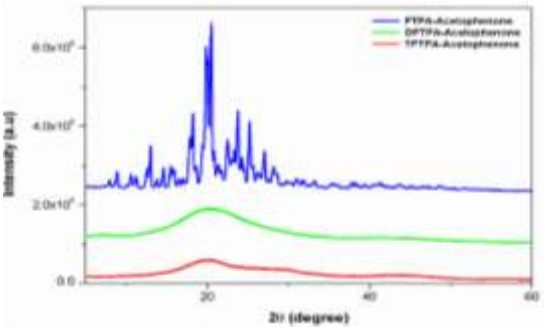

Fig.4. Powder X-ray diffraction patterns of yellow phosphors.

Photophysical properties:

UV - Visible and PL spectra of the synthesized phosphors were measured in dilute CH_2Cl_2 solutions (Fig. 5 & 6). In FTPA-Acetopheneone absorption spectra, the strong absorption peaks at 292 and 416 nm, which are ascribed to the π-π* transitions of conjugated chain [30-32]. Similar observation has been made in the case of N, N, diphenyl-4-styrylaniline where in the molecular structure is very similar to that of FTPA-Acetophenone [29]. The photoluminescence spectra of the FTPA-Acetophenone, DFTPA-Acetophenone and TFTPA-Acetophenone compounds were measured under the monitoring wavelength of 292 and 425 nm, respectively. The emission spectra of phosphors are shown in the Fig.6, which indicates that the FTPA, DFTPA and TFTPA-Acetophenone emits at 558, 535 and 532 nm, respectively.

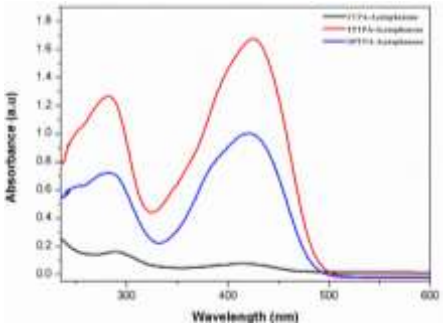

Fig.5. The absorption spectra of TPA substituted Acetophenones in CH_2Cl_2 solvent.

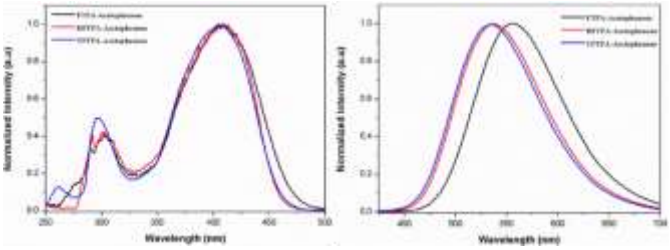

Fig.6. The excitation and emission spectra of TPA substituted acetophenones in CH_2Cl_2 (10^{-4} M).

The photoluminescence quantum yields (PLQY) of the currently synthesized phosphors were tabulated in Table 1. The relative comparison of the PL intensity of the yellow phosphors have been made by keeping the FTPA-Acetophenone emission intensity as one and the calculated relative emission intensity has been tabulated for the DFTPA and TFTPA-Acetophenone in Table.1. The relative intensity of the TFTPA-Acetophenone is 1.58 times higher than that of FTPA-Acetophenone. Solid state photoluminescence studies revealed that the FTPA, DFTPA and TFTPA-Acetophenone phosphors emits at 556, 576, 594 nm, respectively (Fig.7). The observed red shift in the solid state emission can be attributed to the aggregation induced enhanced emission (AIE) [33]. The solvatorchromism of the synthesized phosphors were mentioned in SI.

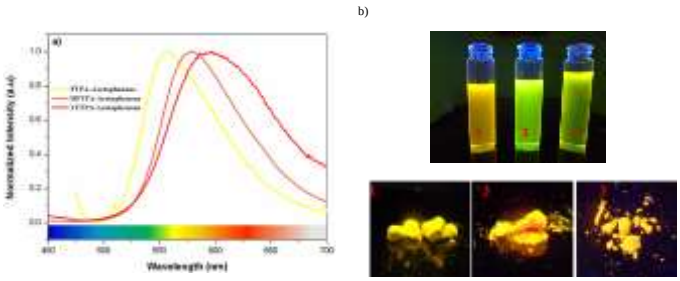

Fig.7. a). The solid state emission spectra of TPA substituted Acetophenones. b) Digital photographs of yellow phosphors in solution and solid state under illumination of UV lamp.

Table 1. Photphysical and CIE chromaticity values of yellow phosphors.

Yellow phosphors	λ_{abs} [a] (nm)	λ_{em} (nm)	PL Intensity comparison	PLQY (Φ)	CIE coordinates (x, y)	
					solution	solid
FTPA-Acetophenone	292, 416	558[a]/ 556[b]	1	0.44	0.4236, 0.5367	0.4562, 0.5002
DFTPA-Acetophenone	284, 420	528[a]/ 578[b]	1.05	0.25	0.2853, 0.5029	0.5202, 0.4660
TFTPA-Acetophenone	282, 423	522[a]/ 594[b]	1.58	0.22	0.2877, 0.4668	0.5504, 0.4393

[a] in CH_2Cl_2 solution, [b] solid

Incorporation of heteroatoms into an organic luminophore, due to intramolecular charge transfer (ICT) which can induce electronic perturbation, such as polarization. This can considerably alter the photophysical properties of the organic phosphor, particularly in color tunability. The AIE of organic phosphor emits in the long wavelength region due to the polarization effect triggered by the D–A interaction (triphenylamine and keto moieties). As shown in Fig. 7, the powders of yellow phosphor emit a yellow light, while in the dilute solution the compounds are showing yellowish green color. Similar observations (AIE in solid state) have been made in the case of Dipyrrolylquinoxaline difluoroborate [36] and Bednzothiazole-enamide [37] complexes.

Cyclic voltammetry studies:

The HOMO and LUMO energy levels of all the phosphor materials can be calculated from the onset oxidation potential (E_{Ox}(onset)) and the onset reduction potential (E_{Red}(onset))

$$HOMO = - [4.4\ V + E_{Ox}\ (onset)]$$

$$LUMO = - [4.4\ V + E_{red}\ (onset)]$$

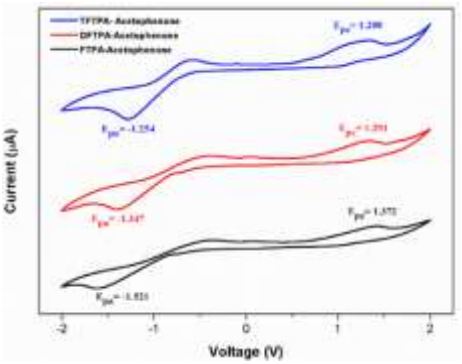

Fig.8. Cyclic voltammetry curves of the three yellow phosphors (E_{pa} and E_{pc} are the cathodic and anodic potential, respectively).

Table 2. Electrochemical data and theoretical HOMO– LUMO gaps.

Yellow phosphors	E_{red}^{onset} (V)	E_{oxd}^{onset} (V)	HOMO [c](eV)	LUMO [c](eV)	Energy gap (ΔE, eV)
FTPA-Acetophenone	-1.521	1.372	-5.772	-2.879	2.89
DFTPA-Acetophenone	-1.347	1.291	-5.691	-3.052	2.63
TFTPA-Acetophenone	-1.254	1.208	-5.608	-3.145	2.46

Fig, 8 shows that all phosphor materials exhibit two reversible oxidation process in the anodic sweep. No reduction signal was detected for any of the phosphors during cathodic scan. The HOMO levels determined from Eonset for FTPA-Acetophenone (-5.7721 eV) was notably higher than that of DFTPA (-5.6915 eV) and TFTPA-Acetophenone (-5.6085 eV). These data shows that the incorporation of acceptor groups from one to three on TPA moiety have great impact on the HOMO and LUMO levels. More specifically, the HOMO and LUMO level values are gradually decreases and increases, respectively (Table. 2). Overall energy gap of the phosphor materials decreases with uniform manner. By contrast, the HOMO level of DFTPA and TFTPA-Acetophenone decreases to ~0.1 eV, which lower than FTPA-Acetophenone, reflecting the fact that the outer acetophenone units are electron-withdrawing nature through an inductive or π-polarization effect.

Lifetime measurements:

Lifetime decay curve analysis of phosphors are shown in the Figure 9. The measured data was fitted with the single exponential function given by the equation $(t) = I_0 + A_1 \exp(-t/\tau)$, where A1 is the scalar quantity obtained from the curve fitting, I0 = 0 is the offset value, t is the time in ms and τ is the decay time value for the exponential component. The luminescent lifetime values (τ) of phosphors FTPA-Acetophenone, DFTPA-Acetophenone and TFTPA-Acetophenone were found to be 3.91, 9.88 and 2.40 μs, respectively.

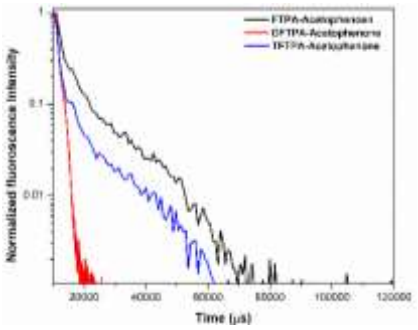

Fig. 9. Lifetime measurements of yellow phosphors.

Computational studies of FTPA, DFTPA and TFTPA-Acetophenone:

Optimized geometries of FTPA, DFTPA and TFTPA-Acetophenone phosphors are given in Fig 10. Their corresponding Frontier orbital energies and gas phase UV-Vis spectral wave lengths are tabulated in Table 3. The frontier orbital (LUMO+1 to HOMO-1) diagrams of all the phosphors are also presented in supplementary information (Figure S1). The Computed Vertical Transitions and Their Oscillator Strengths and Configurations are mention in supplementary information (ST1). The comparison of HOMO – LUMO energy gaps of the phosphor materials in theoretical and experimental are shown in fig.10.

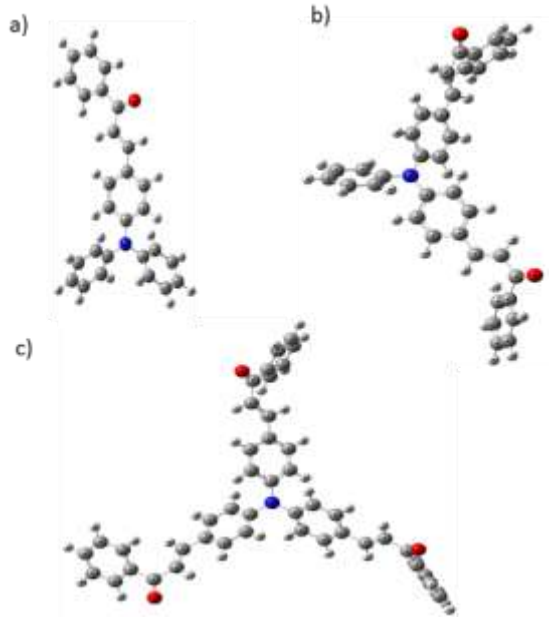

Fig.10. Optimized geometries of (a) FTPA, (b) DFTPA and (c) TFTPA-Acetophenone.

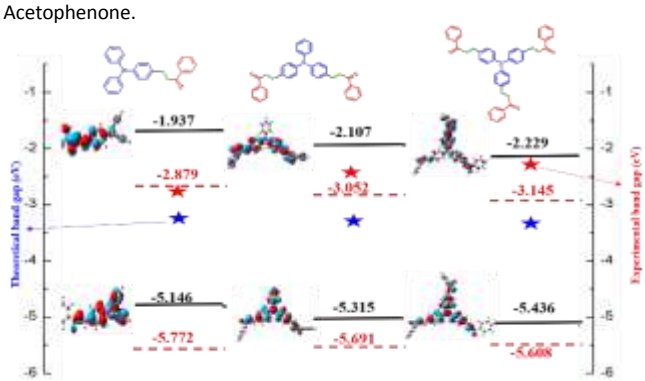

Fig.11. HOMO – LUMO energy gap diagram of yellow phosphors.

The HOMO-LUMO energy gap of TFTPA-Acetophenone is less than that of FTPA-Acetophenone which suggests that there will be bathochromic shift. This is exactly happened when we see the gas phase UV-vis spectral wavelength values from Table 1. But the situation is different when we see the DCM solvent phase UV-vis results. Fig 12(b) depicts the DCM solvent phase UV-vis spectra for FTPA, DFTPA and TFTPA- Acetophenones. Here for FTPA molecule two distinct peaks have been found at 308 and 457 nm. As we move from FTPA to DFTPA it is expected that there will be red shift but small blue shift occurs in first peak at 305 nm and the second one shifted towards red (459 nm). For TFTPA first peak appears at 309 nm and second peak at 456 nm indicates the red shift and blue shift respectively in compare to FTPA and DFTPA- Acetophenones. This results matches with experimental finding given in Fig 5. To see the solvent effect on absorption spectra for these phosphors we took FTPA and calculate the UV-vis spectra with five different solvents like THF, chloroform, DCM, toluene and acetonitrile. The corresponding plot is presented in Fig 12(c). For all the cases two distinct peaks appear in the UV-vis spectra, for example in the case of Toluene solvent, the peaks appear at 305 and 448 nm. The peaks are gradually red shifted if the solvent polarity changes. The order is as follows Toluene < Chloroform < THF < DCM < Acetonitrile.

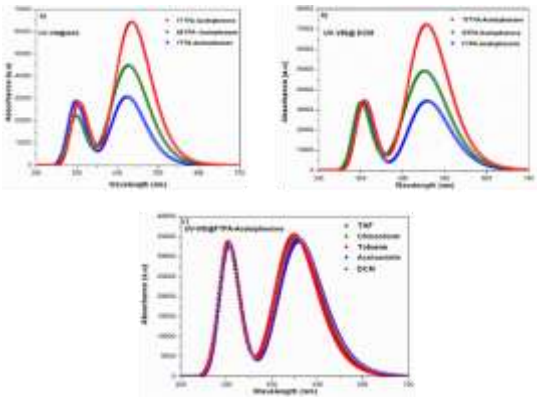

Fig.12. UV-Vis spectra of (a) FTPA, DFTPA, TFTPA-Acetophenones in gas phase (b) in DCM solvent phase and (c) FTPA- Acetophenone in different solvent phase.

Table 3. Calculated absorption (gas phase), HOMO, LUMO, Singlet and triplet energy levels of of the phosphors in CH_2Cl_2 media at TD-DFT/B3LYP level.

Yellow phosphors	HOMO (eV)	LUMO (eV)	Energy gap (ΔE, eV)	λ_{abs}(nm) (Gas phase)	Singlet energy (S_1) (eV)	Triplet energy (T_1) (eV)
FTPA-Acetophenone	-5.146	-1.937	3.209	293, 423	2.716	2.047
DFTPA-Acetophenone	-5.315	-2.107	3.208	299, 433	2.671	2.072
TFTPA-Acetophenone	-5.436	-2.229	3.207	305, 435	2.689	2.117

Singlet (S1) and Triplet (T1) energy levels:

In order to utilize the phosphor as a host material for red emitting organo-phosphors (Iridium or Europium based molecular complexes), it is necessary to know the triplet energy level values. Singlet and triplet energies of the currently synthesized organic phosphors were calculated by using TD-DFT/B3LYP approach. The corresponding energies of the organic phosphors are tabulated in Table 3. The calculated triplet energy level values for the currently synthesized yellow phosphors are in the range of 2.0 to 2.1 eV and it is well match with the known host material Alq_3 [38].

White light emission under fluorescence microscope and CIE Color coordinates:

In order to evaluate the white light emission and suitability to be used in WLEDs, the organic phosphors were excited under blue photons in the fluorescence microscope and the pictures are shown in Fig. 13. One can clearly observe that all the phosphors are emitting white light under blue ray excitation and we believe that the currently synthesized phosphors are suitable for WLEDs.

Fig.13. Phosphors ((a) FTPA-, (b) DFTPA-, (c) TFTPA-Acetophenone under blue ray excitation.

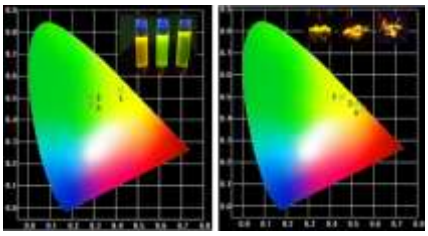

Fig.14. CIE color coordinates of (1) FTPA-, (2) DFTPA-, (3) TFTPA-Acetophenone phosphor materials in solution and solid.

The CIE chromaticity coordinates of the synthesized phosphors and the corresponding emission intensities are tabulated in supplementary information (ST3). The CIE color coordinate of the currently synthesized phosphors show higher color saturation with yellowish-green and yellow color (Fig. 14).

Conclusion:

In summary, we have successfully synthesized a series of triphenylamine with multiple acceptors yellow organic phosphors and demonstrated that the increasing the acceptor groups will leads to red shift in the emission spectrum (yellow to yellowish orange color, due to the π – π interaction and aggregation induced emission). The solvent dependent photoluminescence studies (solvatochromism) were carried out for all the three yellow phosphors and the spectra data's were interpreted in terms of the Lippert–Mataga equation All phosphors thermally stable up to 300°C, it clearly indicates that all the phosphors are useful for the fabrication of white LEDs/OLEDs. These outcomes offer a great platform for the development of practical lighting hybrid devices based on purely organic phosphors.

Acknowledgements:

This work is funded by the Department of Science and Technology (DST), Government of India INSPIRE award no IFA12-CH-48 (VS) and IFA14-CHE-151 (SG).

References

1 a) C. J. Humphreys, *MRS Bull*. 2008, 33, 459-470; b) R. Haitz, J. Y. Tsao, *Phys. Status Solidi A*., 2011, 208, 17 - 29.
2 S. Nakamura, T. Mukai, M. Senoh, *J. Appl. Phys*., 1994, 76, 8189 - 8191.
3 Y.Q.Li, G.de With, H.T Hentzen, *J. Lumin*., 2006, 116, 107-116.
4 T.Kanou, *Handbook of phosphors* (ohm, Tokyo, 1987).
5 a). Yiting Zhu and Nadarajah Narendran, *Jpn. J. Appl. Phys.,* 2010, 49, 100203. b). Yu-Ho, Jang, Ho Seong; Cho, Kyoung Woo; Song, Yong Seon; Jeon, Duk Young; Kwon, Ho Ki, *Optics Letters*, 2009, 34, 1-3.

6 a). W. Ding, J. Wang, M. Zhang, Q. Zhang, Q. Su, *J. Solid State Chem*., 2006, 179, 3582-3585. b). Philipp Pust Volker Weiler, Cora Hecht, Andreas Tücks, Angela S. Wochnik,Ann-Kathrin Henß, Detlef Wiechert, Christina Scheu, Peter J. Schmidt, Wolfgang Schnick, *Nature materials*., 2014, 13, 891 – 896. c). S. Lee, T. Chan and T. Chen., *ACS Appl. Mater. Interfaces*, 2015, 7, 40 – 44, d). H. Zhu Chun, Che Lin, Wenqin Luo, Situan Shu, Zhuguang Liu, Yongsheng Liu, Jintao Kong,En a,Yongge Cao,Ru-Shi Liu & Xueyuan Chen, *Nat. commu*., 5, 4312-4328.

7 Y. Li, A. Delsing, G. With, H. Hintzen, *Chem. Mater*., 2005, 17, 3242-3248.

8 H. Kim, J. Jin, Y. Lee, S. Lee, C. Hong, *Chem. Phys. Lett*., 2006, 431, 341-345.

9 P. Schlotter , R. Schmidt, J. Schneider, *Appl. Phys. A*., 1997, 64, 417-418.

10 F. Hide, P. Gozodoy, S. P. DenBaars, A. J. Heeger, *Appl. Phys. Lett*., 1997, 70, 2664-2666.

11 C. Zhang, A. J. Heeger, *J. Appl. Phys*., 1998, 84, 1579-1582.

12 R. W. Martin, P. R. Edwards, R. Pecharroman-Gallego, C. Liu, C. J. Deatcher, I. M. Watson, K. P. O'Donnell, *J. Phys. D: Appl. Phys*., 2002, 35, 604.

13 G. Heliotis, G. Itskos, R. Murray, M. D. Dawson, I. M. Watson, D. D. C. Bradley, *Adv. Mater*., 2006, 18, 334-338.

14 G. Heliotis, P. N. Stavrinou, D. D. C. Bradley, E. Gu, C. Griffin, C. W. Jeon, M. D. Dawson, *Appl. Phys. Lett*., 2005, 87, 103505-103505-3.

15 E. Gu, H. X. Zhang, H. D. Sun, M. D. Dawson, A. R. Mackintosh, A. J. C. Kuehne, R. A. Pethrick, C. Belton, D. D. C. Bradley, *Appl. Phys. Lett*., 2007, 90, 031116-031116-3.

16 R. Smith, B. Liu, J. Bai, T. Wang, *Nano Lett*., 2013, 13, 3042-3047.

17 Z. Yue, Y. F. Cheung, H. W. Choi, Z. Zhao, B. Zhong Tang, K. S. Wong, *Opt. Mater. Express*., 2013, 3, 1906-1911.

18 N. Laurand, B. Guilhabert, J. McKendry, A. E. Kelly, B. Rae, D. Massoubre, Z. Gong, E. Gu, R. Henderson, M. D. Dawson, *Opt. Mater. Exp*., 2012, 2, 250-260.

19 H. Chun, C.-J. Chiang, A. Monkman, D. O. O'Brien, *J. Lightwave Technol.,* 2013, 31, 3511-3517.

20 A. Hagfeldt, G. Boschloo, L. Sun, L. Kloo and H. Pettersson, , *Chem. Rev*., 2010, 110, 6595-6663.

21 a) C.C. Haung, H.F Meng, G. K. Ho, C.H. Chen, C.S. Hsu, J. H. Huang, S.F. Horng, B. X. Chen, L. C. Chen, *App. Phy.Lett.,* 2004, 84, 1195. b) Q.Wang, J. Ding, D. Ma, Y. Cheng, L. Wang, F. Wang, *Adv. Mater*., 2009, 21, 2397. c) Y.-S. Park, J. W. Kang, D. M. Kang, J. W. Park, Y.-H. Kim, S.-K. Kwon, J.-J. Kim, *Adv. Mater*., 2008, 20, 1957. d) B. W. D' Andrade, R. J. Holmes, S.R. Forrest, *Adv. Mater*., 2004, 16, 624.

22 a) Ju Mei, Nelson L. C. Leung, Ryan T. K. Kwok, Jacky W. Y. Lam, and Ben Zhong Tang *Chem. Rev*. 2015, 115, 11718−11940. B) Ju Mei , Yuning Hong , Jacky W. Y. Lam , Anjun Qin , Youhong Tang , and Ben Zhong Tang, *Adv. Mater*. 2014, 26, 5429–5479

23 a) Thaksen Jadhav, Bhausaheb Dhokale, Shaikh M. Mobin and Rajneesh Misra, *J. Mater. Chem. C*, 2015, 3, 9981. b) Thaksen Jadhav, Bhausaheb Dhokale, Yuvraj patil and Rajneesh Misra, *RSC Adv*., 2015, 5, 68187.

24 a)M. Liang and *J. Chen, Chem. Soc. Rev*., 2013, 42, 3453-3488. b) Ramesh Maragani, Prabhat Gautam, Shaikh M. Mobin and Rajneesh Misra, *Dalton Trans*., 2016, 45,4802. c) T. Sheshashena Reddy, Ramesh Maragani, Bhausaheb Dhokale, Shaikh M. Mobinand Rajneesh Misra, *RSC Advance*, 2016, 6, 7746-7754.

25 L. A. Estrada and D. C. Neckers, *Org. Lett*., 2011, 13, 3304-3307.

26 Rajneesh Misra, Ramesh Maragani, Biswarup Pathak, Prabhat Gautam and Shaikh M. Mobin, RSC Advance, 2016, 5, 71046-71051. b) Rajneesh Misra, a Ramesh Maragani,a K. R. Patelb and G. D. Sharma, RSC Advance, 2014, 4, 34904. c) Rajneesh Misra, Ramesh Maragani, Prabhat Gautam, Shaikh M. Mobin, Tetrahedron Letters 2014, 55, 7102–7105.

27 Chien-Hsin Yang, Han-Lung Chen, Yao-Yuan Chuang, Chun-GueyWu, Chiao-Pei Chen, Shao-Hong Liao, Tzong-LiuWang, *Journal of Power Sources.,* 2009, 188, 627–634.

28 a) Becke, A. *J. Chem. Phys*. 1993, 98, 5648; Lee, C.; b) Yang, W.; Parr, R. G, *Phys. Rev. B*., 1998, 37, 785-789.

29 a). Bauernschmitt, R.; Ahlrichs, R. *Chem. Phys. Lett*., 1996, 256, 454−464. b). Scalmani, G.; Frisch, M. J.; Mennucci, B.; Tomasi, J.; Cammi, R.; Barone, V. *J. Chem. Phys*., 2006, 124, 094107(1−15).

30 Tomasi, J.; Mennucci, B.; Cammi, R. Quantum Mechanical Continuum Solvation Models, *Chem. Rev*., 2005, 105, 2999−3093.

31 Gaussian 09, Revision D.01, M. J. Frisch et.al. Gaussian, Inc., Wallingford CT, 2009.

32 Liming Zhang, Bin Li, Bingfu Lei, Ziruo Hong, Wenlian Li, *J. Lumin*., 128 (2008) 67–73.

33 Rachod Boonsin, Geneviève Chadeyron, Jean-Philippe Roblin, Damien Boyer and Rachid Mahiou, *J. Mater. Chem. C*., 2015, 3, 9580-9587.

34 N. Armroli, L. De Cola, V. Balzami, J.P. Sauvage, C.D. Dietich Buchecker, J.M. Kern, *J. Chem. Soc. Faraday Trans*., 1992, 88, 553-556.

35 Yuning Hong, Jacky W. Y. Lam and Ben Zhong Tang, *Chem. Soc. Rev*., 2011, 40, 5361–5388.

36 Q. Liu, X. Wang, H. Yan, Y. Wu, Z. Li, S. Gong, P. Liu and Z. Liu, *J. Mater. Chem. C.*, 2015, 3, 2953-2959.

37 Y. Hong, J. W. Y. Lam and B. Z. Tang, *Chem. Commun*., 2009, 4332-4353.

38 Ta – Ya chu, Yao – Shan Wu, Jenu – frang Chen, Chin H. Chen, *Chem. Phy. Lett.,* 2005, 404, 121 - 125.